Alternate Paths from Epidermal Growth Factor Receptor to Akt in Malignant Versus Nontransformed Lung Epithelial Cells

ErbB3 Versus Gab1

Gunamani Sithanandam, George T. Smith, Janet R. Fields, Laura W. Fornwald, and Lucy M. Anderson

Basic Research Program, SAIC-Frederick, Frederick, Maryland; and Laboratory of Comparative Carcinogenesis, National Cancer Institute at Frederick, Frederick, Maryland

In many human lung adenocarcinoma cell lines, a pathway involving epidermal growth factor receptor (EGFR), ErbB2 and ErbB3 receptors, phosphatidyl inositol 3-kinase (PI3K), Akt, glycogen synthase kinase 3-β (GSK3-β), and cyclin D1 controls cell growth, survival, and invasiveness. We have investigated this pathway in paired transformed/nontransformed cell lines from murine peripheral lung epithelium, E9/E10 and A5/C10. The E9 and A5 carcinoma lines expressed ErbB3 and transforming growth factor-α (TGF-α) and responded to TGF-α stimulation with protein complex formation including the p85 regulatory subunit of PI3K, activation of Akt, phosphorylation of GSK3-β, and increased cyclin D1 protein and the cell cycle. ErbB3 and TGF-α were not detected in the nontransformed E10 and C10 cell lines. Nevertheless, exposure of E10 or C10 cells to TGF-α activated PI3K and Akt and increased cyclin D1 and cell growth. The effector pathway from the EGFR to PI3K in these nontransformed cells included the adaptor Grb2, the docking protein Gab1, and the phosphatase Shp2. Gab1 was highly expressed in E10 and C10 cells but not in the malignant E9 and A5 sister lines. Complexes of EGFR/Grb2/Gab1/Shp2 after TGF-α stimulation were prominent only in E10 and C10 cells. Thus, alternate pathways downstream of EGFR regulate mitosis in these paired malignant versus nontransformed lung cell lines.

Keywords: EGFR; ErbB3; Gab1; Akt; lung epithelial cells

Complex interactions of growth factors, receptors, and signaling pathways regulate normal cell division of lung epithelial cells and, in their derangement, contribute to the development of malignancy. Systematic distinction of essential from secondary changes is facilitated by the availability of two pairs of cell lines derived from cells of the peripheral lung epithelium of BALB/c female mice, which grew out after explanting the lungs (1, 2). Each of these pairs was derived from a single immortalized cell line, one subline of which underwent spontaneous malignant transformation to an adenocarcinoma line showing growth in soft agar and as nude mouse xenografts. These pairs are designated E9/E10 and A5/C10, where E9 and A5 are the malignant lines.

The presence of lamellar bodies and cytoskeletal features indicated that type II cells may have been the origin of these lines (1, 2), confirmed by specific staining with antibodies to cytokeratins (3). We have confirmed lamellar body–like structures in E10 and C10 cells by electron microscopy (unpublished data). E10 and C10 present 2–5% S-phase cells at confluence, compared with 20–30% of E9 and A5 cells (3). The two nontransformed cell lines, compared with the two transformed lines, have higher levels of fibronectin, laminin, and vitronectin; more organized cytoskeletons; more numerous gap junctions; and more glucocorticoid- and platelet-derived growth factor receptors (3).

We have used these paired lines to investigate mechanisms of regulation of cell growth via the epidermal growth factor receptor (EGFR) ErbB1 in malignant compared with nontransformed peripheral lung epithelial (PLE) cells. The EGFR family of receptors can regulate many aspects of cellular behavior, including proliferation (4, 5). This family consists of four members—ErbB1 (EGFR), ErbB2, ErbB3, and ErbB4—which have a common structural design involving an extracellular ligand-binding domain, a single hydrophobic transmembrane domain, and a tyrosine kinase cytoplasmic domain. Ligands include epidermal growth factor (EGF) and transforming growth factor-α (TGF-α) for the EGFR and heregulins for ErbB3 and ErbB4. However, no direct ligand has been discovered for ErbB2, and ErbB3 lacks intrinsic kinase activity. Thus, heterodimerization among the ErbB family members is central to their functioning.

With regard to peripheral lung, immunohistochemical studies have indicated the presence of EGFR (6) and ErbB3 (7, 8) in normal human adult type II pneumocytes but have indicated the absence of ErbB2 (7, 9). Immunohistochemistry and RNA analyses indicate a lack of EGF in these cells (6, 10). The ErbB receptors are frequently upregulated in non-small cell lung cancers. The EGFR may have high levels of expression (11), and ErbB2 is overexpressed in up to 100% of lung adenocarcinomas with associated poor prognosis (12). ErbB3 was highly expressed in some lung adenocarcinomas (13) with associated poor prognosis (8), and ErbB3 co-expression with other family members indicated probability of tumor recurrence (14). In other types of cancer, including mammary and ovarian, complex with ErbB3 greatly enhances signaling through ErbB2 (15, 16).

These observations prompted our examination of ErbB3 expression and signaling in human lung adenocarcinoma cell lines. We observed that ErbB3 was highly expressed in five of seven human lung adenocarcinoma cell lines but absent from an immortalized nontransformed human cell line, HPL1D, derived from peripheral lung epithelium (17). Further studies showed that a signaling pathway involving EGFR, ErbB2, ErbB3, phosphatidylinositol 3-kinase (PI3K), Akt, glycogen synthase kinase 3- β (GSK3-β), and cyclin D1 is essential for the maintenance of survival, mitosis, and invasiveness of these cells (17, 18). However, because only one nontransformed cell line from human lung peripheral epithelium was available, the generality of the conclusions could not be confirmed. These results are extended here by use of the E9/E10 and A5/C10 paired cell lines.

(*Received in original form February 1, 2005 and in final form July 14, 2005*)

This project has been funded in part with federal funds from the National Cancer Institute under contract no. NO1-CO-12400.

Correspondence and requests for reprints should be addressed to Gunamani Sithanandam, Basic Research Program, SAIC-Frederick, Building 538, Ft. Detrick, Frederick, MD 21702. E-mail: sithanan@ncifcrf.gov

Am J Respir Cell Mol Biol Vol 33. pp 490–499, 2005
Originally Published in Press as DOI: 10.1165/rcmb.2005-0049OC on July 29, 2005
Internet address: www.atsjournals.org

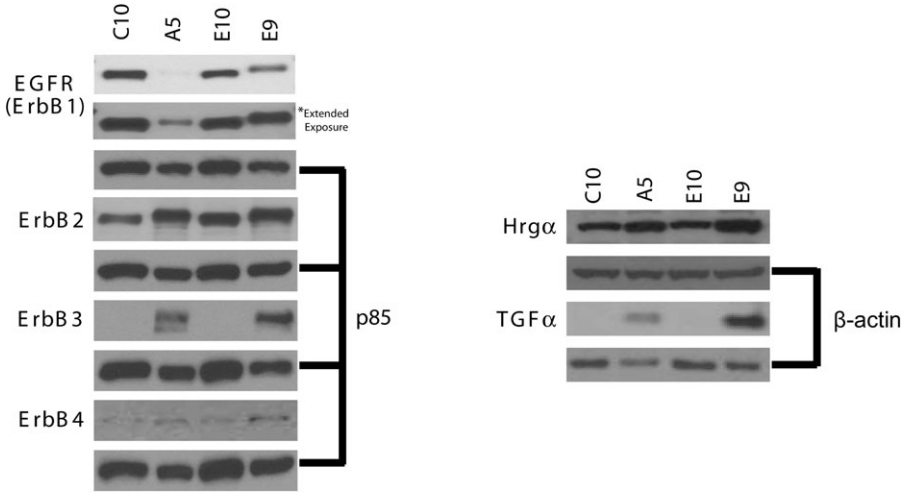

Figure 1. Expression of ErbB family members and ligands in nontransformed (C10, E10) and malignant (A5, E9) sister lung cell lines. Western blots of lysates (50 μg protein for growth factor receptors and 20 μg protein for growth factors) were probed with antibodies as indicated. Sizes of the bands shown are 170 kD (EGFR), 185 kD (ErbB2), 185 kD (ErbB3), 180 kD (ErbB4), 18 kD (TGF-α), and 44 kD (Hrg-α). P85 was used as a loading control for growth factor receptors (6% gel), and β-actin was used as a loading control for growth factors Hrg-α (12% gel) and TGF-α (4–20% gradient gel). An extended exposure of the blot was used to confirm the low level of expression of EGFR in A5 cells (*left panel*, *second row*).

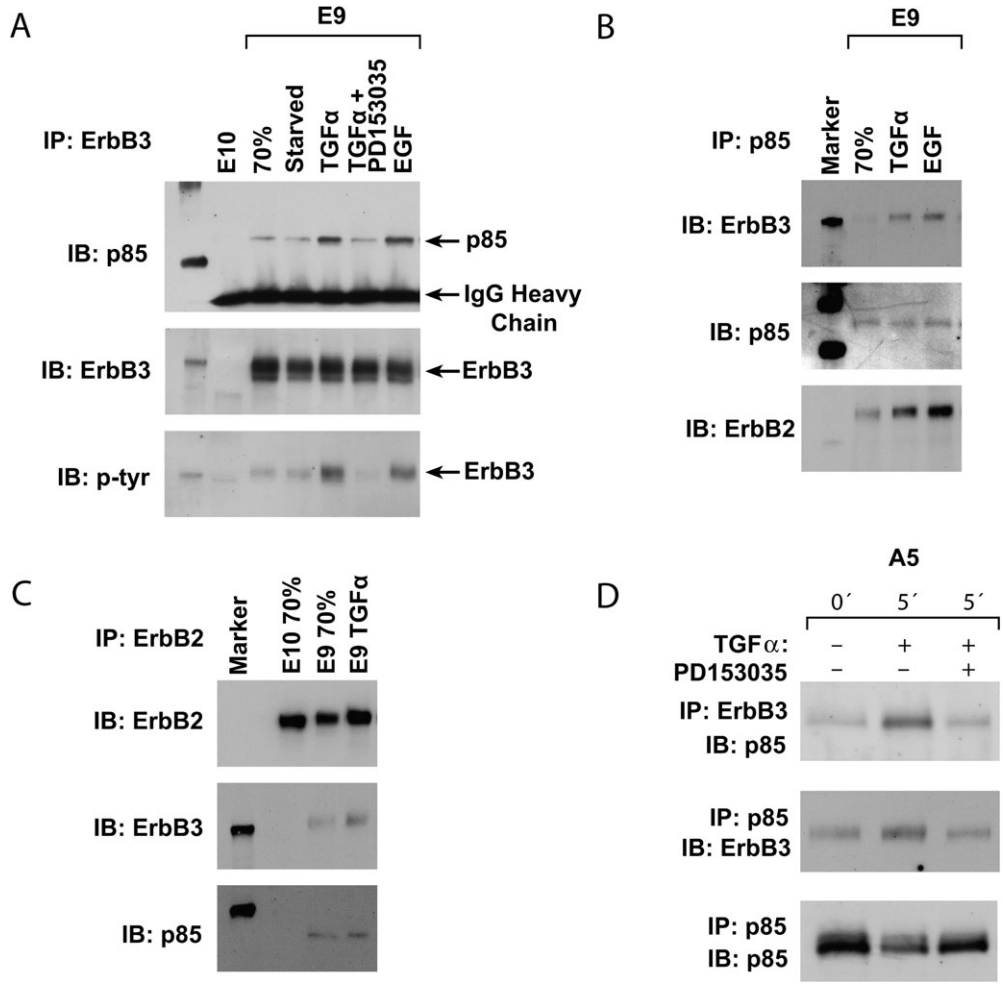

Figure 2. Stimulation of ErbB2/ErbB3/PI3K complex formation by TGF-α in lung adenocarcinoma cells. (*A*) E10 and E9 cell lysates were immunoprecipitated with anti-ErbB3 and were immunoblotted with anti-PI3K p85, then after stripping immunoblotted sequentially with anti-ErbB3, and antiphosphotyrosine. E10 cells were used at 70% confluence. E9 cells were studied at 70% confluence or at 70% confluence and serum starved for 48 h or after treatment of serum-starved cells with TGF-α (with or without EGFR inhibitor PD153035) for 5 min or after treatment of serum-starved cells with EGF. (*B*) E9 cells at 70% confluence or cells serum starved and treated with TGF-α or EGF were immunoprecipitated with anti-p85 and immunoblotted with anti-ErbB3, then after stripping, immunoblotted sequentially with anti-p85 and anti-ErB2. (*C*) E9 and E10 cells at 70% confluence and E9 cells treated with TGF-α after serum starvation were immunoprecipitated with anti-ErbB2 and were immunoblotted with anti-ErbB2 then after stripping immunoblotted sequentially with anti-ErbB3 and anti-p85. (*D*) A5 carcinoma cells were serum starved and treated with TGF-α for 5 min with or without the PD153035 inhibitor. Immunoprecipitation/immunoblotting assays with anti-ErbB3 and anti-p85 were performed as indicated.

With these paired cells lines, we provide evidence that in the nontransformed lines uniquely, EGFR signals to Akt using the scaffolding adapter Gab1 (Grb2 associated binder 1) and the protein tyrosine phosphatase Shp2 (SH2 containing protein tyrosine phosphatase 2). On the other hand, we have confirmed operation of the EGFR/ErbB3/Akt pathway in the carcinoma lines but not in the nontransformed lines. Alternate routing of downstream mitogenic signaling from EGFR may be a characteristic of lung adenocarcinoma.

MATERIALS AND METHODS

Cell lines from peripheral mouse lung epithelium, originally derived as described (1, 2), were obtained from Dr. R. Ruch, Medical College of Ohio (E10), Dr. A. Malkinson, University of Colorado (E9), and Dr. S. Jakowlew (National Cancer Institute) (C10 and A5). E10 and E9 cells were maintained in CMRL 1066 basal medium. C10 and A5 cells were maintained in Dulbecco's modified Eagle's medium (Biofluids, Rockville, MD) and were supplemented with 2 mM glutamine, penicillin/streptomycin, and 10% fetal calf serum (PAA Laboratories, Parkerford, PA).

For serum starvation experiments, 70% confluent cultures were maintained in media with 0.1% serum for 48 h and rinsed with fresh 0.1% serum-containing media 2 h before the experiment. Human EGF was obtained from Invitrogen (Carlsbad, CA), and TGF-α was obtained from Upstate Biotechnology (Lake Placid, NY). PD153035 (1 μM), a specific inhibitor of EGFR (CalBiochem, San Diego, CA), or LY294002 (25–50 μM), a specific inhibitor of PI3K (Sigma, St. Louis, MO) was added 30 min before the addition of TGF-α (20 ng/ml) or EGF (100 ng/ml). Antibodies to EGFR, ErbB2, EGF, TGF-α, heregulin-α (Hrg-α), Grb2, Shp2, and total GSK3-β kinase were from Santa Cruz Biotechnology (Santa Cruz, CA); antibodies to ErbB3, phospho-specific EGFR, phospho-specific ErbB2, phosphotyrosine (clone 4G10), PI3K p85α (mouse monoclonal, clone UB93-3), polyclonal p85, Gab1, Gab2, and cyclin D1 were from Upstate Biotechnology; and antibodies to Akt, phospho-Akt, and phospho-GSK3-β were from Cell Signaling Technology (Beverly, MA).

Cultured cells for immunoblots or immunoprecipitations were rinsed with cold phosphate buffered saline (PBS) (17 mM KH_2PO_4, 50 mM Na_2HPO_4, and 150 mM NaCl) and scraped in lysis buffer containing 20 mM Tris (pH 7.5), 150 mM NaCl, 1 mM EDTA, 1 mM EGTA, 1% Triton X-100, 2.5 mM sodium pyrophosphate, 1 mM β-glycerophosphate, 1 mM sodium orthovanadate, and 1 μg/ml Leupeptin (Cell Signaling Technology) and supplemented with 1 mM phenylmethylsulfonyl fluoride (Sigma) just before use. For immunoprecipitation, cells were prepared in lysis buffer as described previously, and 500 μg of protein was immunoprecipitated with antibodies overnight at 4°C. Protein A or G agarose (Roche Molecular Biochemicals, Indianapolis, IN) was added, and incubation continued for 2 h at 4°C. The immunoprecipitates were washed three times in lysis buffer before electrophoresis and immunoblotting.

For immunoblotting, the cell lysates were mixed with 2× Laemmli sample buffer and loaded at the protein concentrations indicated in the figure legends on Tris-Glycine gels (Invitrogen): 6% gels for growth factor receptors; 16% gels or 4–20% gradient gels for TGF-α growth factor; and 12% gels for Akt, GSK3-β, Grb2, Hrg-α, and cyclin D1. Lysates were electrophoresed at 100 V. After transfer to Hybond nitrocellulose membranes (Amersham, Buckinghamshire, UK) at 22 V at room temperature, the blots were blocked in 3% bovine serum albumin or 3–5% dried milk for 2 h at room temperature and probed overnight with antibodies at 1:1,000 dilution (1:100 dilution for monoclonal anti-p85α). After application of appropriate secondary antibody (Amersham), an ECL kit (Amersham) was used for the detection of bound antibody. Bands were scanned with a Visioneer one-touch 9,320 scanner (Pleasanton, CA) and quantified with UnScanIt software (Silk Scientific Inc., Orem, UT). For reprobing with another antibody, blots were stripped in buffer containing 100 mM 2-mercaptoethanol, 2% sodium dodecyl sulfate, and 65 mM Tris (pH 6.8) for 30 min at 60°C and washed for 1 h with PBS/0.1% Tween 20.

For flow cytometric analysis (fluorescence-activated cell sorter [FACS]), cells were treated as described in the figure legends, trypsinized (Biosources, Rockville, MD), washed twice with ice-cold PBS, resuspended in PBS, fixed by the addition of absolute ethanol to a final concentration of 70%, and held at −20°C. The day before the FACS analysis, the cells were washed with PBS and resuspended in PBS, and the cell nuclei were stained in the dark with 100 μg/ml propidium iodide (Sigma) containing 125 U/ml RNase and held overnight at −4°C. The next morning, 10,000 stained nuclei were analyzed in a Coulter XL flow cytometer, using System II version 3.0 software to ascertain percentage of cells in the G_0/G_1, S, and G_2/M phases of the cell cycle based on the DNA content characteristic of each of these phases. Significances of differences were evaluated with parametric or nonparametric tests as appropriate with software from SigmaPlot, Inc., and GraphPad, Inc., Instat Version 3.00.

All results shown are representative of at least three independent experiments with different cell cultures.

Figure 3. Effects of TGF-α on PI3K p85, Akt, GSK3-β, and cyclin D1 in all cell lines. (*A*) C10, A5, E10, and E9 cell lines at 70% confluence were serum starved and treated with TGF-α for 5 min in the presence or absence of inhibitor PD153035. Lysates were immunoprecipitated with anti-EGFR and immunoblotted with anti-p85. A TGF-α–stimulated, PD153035-inhibited complex was detected in all four lines. (*B*) C10, A5, and E10 cells pretreated with or without the inhibitor PD153035 were stimulated for 5 min with TGF-α. Lysates from these cells were immunoprecipitated with anti-ErbB2 and immunoblotted with anti-p85. (*C*) The four cell lines were treated as described previously for 5 or 10 min and immunoblotted, with sequential stripping, for EGFR, pEGFR, Akt, and pAkt. EGFR and Akt phosphorylations were observed in all four lines in response to TGF-α and were inhibited by PD153035. (*D*) The four cell lines were treated as described previously for intervals between 10 min and 6 h with or without the PD153035 inhibitor of EGFR or LY294002 specific for PI3K and immunoblotted for total Akt and pAkt. Total Akt did not change. Akt phosphorylation reached a maximum by 30 min and was markedly reduced by both inhibitors. (*E*) The four cell lines were treated as described previously for 5 or 10 min in the presence or absence of the PD153035 or LY294002 inhibitors and immunoblotted for phosphorylated GSK3-β. In all lines, the latter was increased by TGF-α treatment, and the increase was partially blocked by each inhibitor. (*F*) The four cell lines were treated as described previously for intervals of 30 min to 6 h in the presence or absence of PD153035 or LY294002 and immunoblotted for cyclin D1. The latter increased progressively over this time course, and this increase was completely blocked by each inhibitor.

RESULTS

High Expression of ErbB3 and TGF-α in Malignant Lung Cell Lines

Because ErbB3 is highly expressed in the majority of human lung adenocarcinoma cell lines but is not detected in the nontransformed cell line HPL1D from human lung peripheral epithelium (17), we tested whether the same would be true for the paired transformed/nontransformed cell lines from mouse PLE cells E9/E10 and C10/A5. In confirmation of the findings for human lung adenocarcinoma, ErbB3 protein was highly expressed in malignant lines E9 and A5 but was not detected in the nontransformed sister lines E10 and C10 (Figure 1). Thus, upregulation of ErbB3 in lung adenocarcinoma cells seems to be a general phenomenon. By contrast, EGFR levels were higher in the E10 and C10 cells, although EGFR was still detectable in the E9 and A5 cells. ErbB4 was expressed in all four cell lines.

The presence of agonists for the ErbB receptors was investigated. EGF was not detected in any cell line (data not shown). TGF-α was expressed only in the E9 and A5 adenocarcinoma lines (Figure 1). Hrgα was detected in all lines.

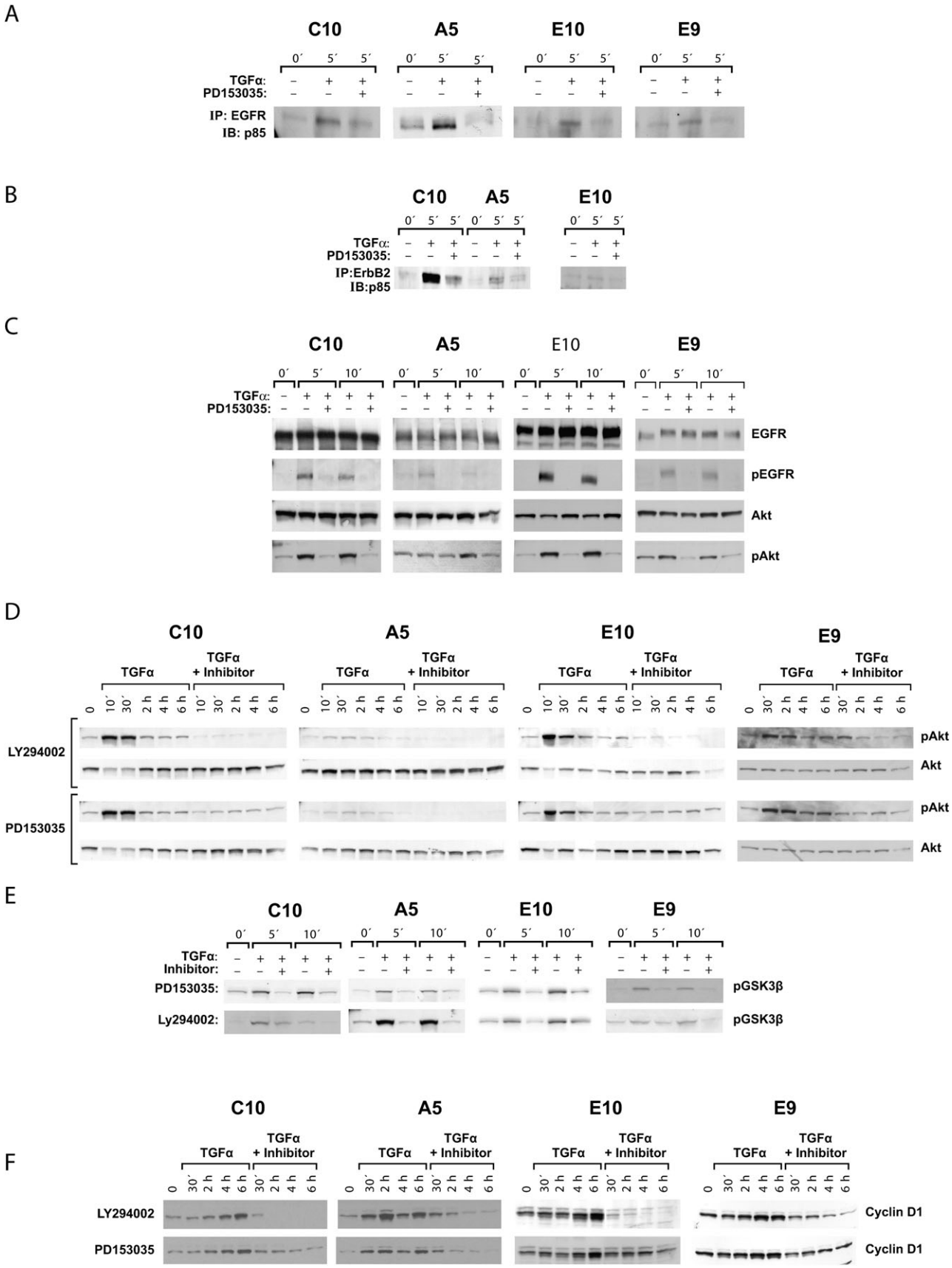
A
C10
A5
E10
E9
0′ 5′ 5′
TGFα:
PD153035:
IP: EGFR
IB: p85
B
C10
A5
E10
0′ 5′ 5′
TGFα:
PD153035:
IP:ErbB2
IB:p85
C
C10
A5
E10
E9
0′ 5′ 10′
TGFα:
PD153035:
EGFR
pEGFR
Akt
pAkt
D
C10
A5
E10
E9
TGFα
TGFα + Inhibitor
0 10′ 30′ 2 h 4 h 6 h
LY294002
PD153035
pAkt
Akt
E
C10
A5
E10
E9
0′ 5′ 10′
TGFα:
Inhibitor:
PD153035:
Ly294002:
pGSK3β
F
C10
A5
E10
E9
TGFα
TGFα + Inhibitor
0 30′ 2 h 4 h 6 h
LY294002
PD153035
Cyclin D1

ErbB2/ErbB3/PI3K p85 Complex in E9 and A5 Cells after EGFR Activation

In previous studies of human lung adenocarcinoma cells, ErbB3 was linked to PI3K downstream, with an ErbB2/ErbB3 heterodimer forming a complex with the p85 regulatory subunit of PI3K (17). To ascertain whether this was true in the mouse lung adenocarcinoma cells, TGF-α or EGF was used to activate EGFR, ErbB2, and ErbB3 after serum starvation. An antibody to ErbB3 was used for immunoprecipitation of E9 cell lysates, followed by immunoblotting for ErbB3, p85, and phosphotyrosine. The results show an increase in p85 and of phosphotyrosine in the complex, which was blocked by inclusion of the EGFR inhibitor PD153035 (Figure 2A). In a complementary experiment, after treatment of serum-starved E9 cells with TGF-α or EGF, antibody to p85 immunoprecipitated ErbB3 and ErbB2 (Figure 2B). Involvement of ErbB2 was confirmed by the presence of ErbB3 and p85 in immunoprecipitates with anti-ErbB2 antibody (Figure 2C). Lack of signal with E10 cells confirmed the specificity of these results (Figures 2A and 2C). These findings were confirmed for the A5 adenocarcinoma cell line, where the occurrence of a TGF-α–stimulated, PD153035-inhibited, ErbB3-p85 complex was demonstrated by reciprocal immunoprecipitation-immunoblotting assays (Figure 2D).

Activation of an EGFR/PI3K/Akt Pathway by TGF-α in Nontransformed Cell Lines

Because EGFR, ErbB2, and ErbB4, but not ErbB3, were detected by Western blotting in the nontransformed E10 and C10 cell lines (Figure 1), we determined whether activation of p85 could be downstream of these receptors. Cell lysates were immunoprecipitated with anti-EGFR and immunoblotted with anti-p85. In E10 and C10, as in E9 and A5, treatment of serum-starved cells with TGF-α resulted in the formation of a complex of EGFR and p85, and the amount of this complex was markedly reduced by the inclusion of the EGFR-specific inhibitor PD153035 (Figure 3A). A complex of ErbB2 and p85 was seen after TGF-α stimulation in C10, A5, and E10 (Figure 3B), as had been shown for E9 (Figures 2B and 2C). Similarly, in all four cell lines, TGF-α treatment led to an increase in pAkt, and this was blocked by treatment with PD153035 (Figure 3C). Increases in PD153035-inhibitable pEGFR were also demonstrated with these lysates (Figure 3C). This was especially prominent in the E10 and C10 cells, with high expression of EGFR. At the same film exposure time, the pEGFR band was fainter in A5 and E9 but was distinctly present (Figure 3C) and was confirmed by longer exposures (data not shown).

PI3K activation of Akt as a result of EGFR stimulation was confirmed for all four lines by use of the PI3K-specific inhibitor LY294002 over a 6-h time course (Figure 3D). pAkt levels were lower in the A5 cells and responded somewhat more slowly to the TGF-α but were clearly present and confirmed by longer film exposure (not shown). Thus, in all four lines, the EGFR was responsive to TGF-α and formed an Akt-activating complex with PI3K/p85.

GSK3-β and Cyclin D1 as Downstream Targets of pAkt in Malignant and Nontransformed Cell Lines

pAkt may regulate the cell cycle by phosphorylation of GSK3-β, resulting in downregulation of this protein and hence increased stability of cyclin D1. Operation of this pathway was noted in human lung adenocarcinoma cells (17, 18). This was confirmed for the mouse E9 and A5 lung adenocarcinoma lines and for the nontransformed E10 and C10 cells. Phosphorylation of GSK3-β was demonstrated in all four cell lines, and this event was sensitive to inhibition by PD153035 and LY294002 (Figure 3E). Also in all four cell lines, levels of cyclin D1 increased steadily up to 6 h after TGF-α treatment; this increase was blocked by treatment with EGFR inhibitor PD153035 or PI3K inhibitor LY294002 (Figure 3F).

EGFR-PI3K Pathway Contribution to Cell-Cycle Control in Malignant and Nontransformed Cell Lines

To confirm that the changes in cyclin D1 indicated differences in cell growth, cell-cycle analysis was performed by FACS for C10, E9, and E10 cells. Serum starvation was followed by TGF-α stimulation. E10 cells recover poorly from complete serum starvation; therefore, they were starved in 1% serum. A5 cells could not be included in this experiment because they show a major apoptotic response to serum starvation. For C10, E9, and E10 cells, serum starvation led to arrest of the cell cycle, with significant increases in G_0/G_1 fractions and decreases in S-phase cells (Table 1). C10 and E10 also experienced a decrease in G_2/M phase cells after starvation. TGF-α treatment resulted in the resumption of cell cycle in all cell lines, as shown by a decrease in G_0/G_1 fractions, although this was of borderline statistical significance for E10 cells. This was accompanied by increase in S-phase cells in E9 and E10, whereas C10 responded to TGF-α with a prominent elevation in the G_2/M fraction. In all three lines, the stimulatory effects of the TGF-α on cell cycle were significantly abrogated by treatment with PD153035 or LY294002, confirming involvement of the EGFR-PI3K pathway.

The reason for the differences in cell-cycle phase distributions in C10 compared with E10 and E9 is not known. C10 cells grow somewhat faster than E10 cells (not shown) and express less p19, p53, and $p21^{WAF1}$ (19). These differences may result in more rapid transit of the S phase of the cell cycle by C10 cells.

Inducible Gab1/p85 Complex in Nontransformed E10 and C10 Cells but Not in E9 or A5 Carcinoma Cells

If ErbB3 connects the EGFR to PI3K/p85 in the carcinoma cells, then how is this connection made in the nontransformed E10 and C10 cells, which lack ErbB3? We postulated that a member of the Gab family (20) could be a candidate for this function. The Gab1 docking protein is known to be recruited to EGFR complexes through the adaptor Grb and in turn to bind to the p85 subunit of PI3K (20, 21). Lysates of C10 and E10 cells responded with a strong signal to anti-Gab1 antibody; much less was detected in E9 and A5 cells (Figure 4A). Furthermore, in TGF-α–stimulated C10 and E10 cells, a mobility shift in Gab1 was noted (consistent with phosphorylation). This shift was not seen in the presence of the EGFR inhibitor PD153035. No such shift occurred in E9 or A5 cells treated with TGF-α. Quantitative assessment showed a 5- to 10-fold difference in Gab1 expression between C10 and A5 and between E10 and E9 (Figure 4B).

Increased association of EGFR with Grb2 was observed in response to TGF-α stimulation in all four cell lines. This association was inhibited with PD153035 treatment in all four cell lines (Figure 4C). Repeated experiments to coimmunoprecipitate EGFR with Gab1 failed to indicate a direct association between EGFR and Gab1 in TGF-α–stimulated cells (data not shown). Immunoprecipitation of these cell lysates with anti-Grb2 antibody confirmed formation of an EGFR-dependent Grb2/Gab1 complex after treatment with TGF-α only in C10 and E10 cells (Figure 4D). Involvement of ErbB2 was also explored. TGF-α stimulated a direct association of Gab1 to ErbB2 only in C10 cells; this complex was absent in E10 cells (Figure 4E). Even with 2 mg protein from E10 cell lysates, there was no detectable association between ErbB2 and Gab1 (data not shown).

TABLE 1. CELL-CYCLE STIMULATION OF MALIGNANT E9 AND NONTRANSFORMED E10 AND C10 CELLS WITH TGFα AND SUPPRESSIVE EFFECTS OF PD153035 AND LY294002 INHIBITORS

	Proliferating	Starved	TGF-α 14 h	T+LY 14 h	T+PD 14 h	TGFα 20 h	T+LY 20 h	T+PD 20 h
E9								
	41.8 ± 1.02	75.0 ± 0.52	62.73 ± 3.1	76.9 ± 0.88	72.57 ± 2.41	61.6 ± 1.99	78.1 ± 0.68	73.3 ± 0.88
G_0/G_1		**$P \leqslant 0.01$***	**$P \leqslant 0.05$†**	**$P \leqslant 0.05$‡**	**$P = 0.05$‡**	**$P \leqslant 0.05$†**	**$P \leqslant 0.05$‡**	**$P = 0.05$‡**
	49.2 ± 1.51	15.4 ± 0.72	25.2 ± 0.40	12.37 ± 0.59	17.83 ± 0.91	26.87 ± 1.58	11.37 ± 0.63	15.06 ± 1.5
S		**$P \leqslant 0.01$***	**$P \leqslant 0.01$†**	**$P \leqslant 0.01$‡**	**$P \leqslant 0.01$‡**	**$P \leqslant 0.05$†**	**$P \leqslant 0.01$‡**	**$P = 0.05$‡**
	9.0 ± 0.72	9.5 ± 0.86	11.4 ± 3.37	10.7 ± 0.31	9.83 ± 0.11	9.03 ± 1.35	10.43 ± 0.22	11.13 ± 1.23
G_2/M		$P = 0.41$*	$P = 0.6$†	$P = 0.8$‡	$P = 0.5$‡	$P = 0.7$‡	$P = 0.35$‡	$P = 0.14$‡
E10								
	73.1 ± 5.64	91.3 ± 1.35				85.6 ± 3.05	92.06 ± 0.96	92.13 ± 1.27
G_0/G_1		**$P = 0.05$***	—	—	—	$P = 0.104$†	$P = 0.12$‡	$P = 0.15$‡
	13.2 ± 2.86	1.5 ± 0.41				4.68 ± 0.39	0.82 ± 0.05	1.58 ± 0.21
S		**$P \leqslant 0.05$***	—	—	—	**$P \leqslant 0.01$†**	**$P \leqslant 0.01$‡**	**$P \leqslant 0.05$‡**
	12.68 ± 2.73	5.75 ± 1.0				8.7 ± 2.3	5.57 ± 1.52	4.84 ± 1.29
G_2/M		**$P = 0.05$***	—	—	—	$P = 0.25$†	$P = 0.218$‡	$P = 0.175$‡
C10								
	53.8 ± 2.8	79.3 ± 2.19				53.8 ± 4.68	84.6 ± 0.59	74.1 ± 3.4
G_0/G_1		**$P \leqslant 0.05$***	—	—	—	**$P \leqslant 0.05$†**	**$P \leqslant 0.05$‡**	**$P \leqslant 0.05$‡**
	25.17 ± 3.34	7.03 ± 1.19				9.3 ± 0.66	1.57 ± 0.03	8.85 ± 0.56
S		**$P \leqslant 0.05$***	—	—	—	$P = 0.06$†	**$P \leqslant 0.01$‡**	$P = 0.74$‡
	30.4 ± 2.69	13.2 ± 1.13				36.2 ± 4.9	13.06 ± 0.63	16.6 ± 1.1
G_2/M		**$P \leqslant 0.05$***	—	—	—	**$P \leqslant 0.05$†**	**$P \leqslant 0.05$‡**	**$P \leqslant 0.05$‡**

The percentages of cells in G_0/G_1, S, and G_2/M phases of the cell cycle as determined by FACS from three different experiments for E9, E10, and C10 are shown. Proliferating cultures were analyzed at 70% confluence, after serum-starvation for 48 h, and after treatment with TGF-α (T) for 14 or 20 h (E9) or 20 h (C10) with or without EGFR inhibitor PD153035 (PD) or PI3K inhibitor LY294002 (LY). TGFα stimulated re-entry of serum-starved cells into the cell cycle, and this was blocked by either inhibitor.

Bold type indicates significant *P* values.

* *P* values for the comparisons, proliferation versus starved cells.

† *P* values for the comparisons, starved versus TGFα-treated cells.

‡ *P* values for the comparisons, TGFα-treated versus TGFα plus inhibitor–treated cells, respectively.

From these results, it seemed possible that the connection between EGFR and p85, provided by ErbB3 in the malignant E9 and A5 cells, could be a function of Gab1 in the nontransformed E10 and C10 cells. This was confirmed: Immunoprecipitates of E10 and C10 lysate with anti-p85 antibody contained Gab1; amounts of immunoblotted Gab1 were especially high in E10 cells. Less Gab1 and a different migration pattern were seen when the EGFR inhibitor PD153035 was used (Figure 4F). Much lower Gab1 signals were observed in A5 cells and were barely detectable in E9 cells (Figure 4F).

In further exploration of these interactions, antibody to phosphotyrosine, which is effective for immunoprecipitation, was used. After TGF-α, there was marked increase in Gab1, which was inhibited by PD153035 (Figure 4G), and Gab2 was detectable. TGF-α also resulted in increased p85 in the complex, with some mobility shift (Figure 4G).

Interaction of Gab1 with Shp2

Gab proteins have essential functional interactions with the protein tyrosine phosphatase Shp2 (20, 21). Immunoprecipitation of C10 and E10 cells with anti-Shp2 antibodies revealed a Gab1 complex that increased after TGF-α and was sensitive to PD153035 inhibition (Figure 5A). There was much less of this complex in E9 cells, and none was detected in A5 cells (Figure 5A). In the reciprocal assay, immunoprecipitation with anti-Gab1 and immunodetection with anti-Shp2 gave similar results (Figure 5C). The p85 subunit of PI3K was also found to be present in the anti-Shp2 complex (Figure 5D).

DISCUSSION

Evidence is increasing for a consistent role for a PI3K-Akt-cyclin D1 pathway in growth of lung cancers, including adenocarcinomas (22–24), implying direct involvement of the EGFR (25, 26). The evidence presented here further extends this body of data to two mouse lung adenocarcinoma cell lines and confirms a malignancy-related role for the receptor ErbB3 in combination with EGFR and ErbB2. Our data establish for the first time the importance of the EGFR-PI3K-Akt-cyclin D1 pathway in proliferation of nontransformed cells from the peripheral lung. Stimulation of cell division in nontransformed type II–like cells in culture by EGF and TGF-α has been demonstrated (27–30). An *in vivo* experiment with a dominant negative EGFR mutant clearly showed the role of this receptor in proliferative responses of the type II cells to lung injury (31). *In vivo*, TGF-α is produced by mesenchymal and inflammatory cells after injury. Our E10 and C10 cells, however, had no detectable EGF or TGF-α. What stimulates the EGFR in these cells during proliferation in subconfluent cultures remains to be determined; heparin-binding EGF, amphiregulin, betacellulin, and decorin are possibilities.

Activation of Akt as a result of EGFR stimulation in nontransformed PLE cells is shown here possibly for the first time. The PI3K-Akt pathway was activated in rat primary lung type II cells by surfactant-associated protein A and was associated with upregulation of anti-apoptotic pathways; proliferative effects were not measured (32). A role for Akt activation was shown in the stimulation of proliferation of rat lung type II cells by keratinocyte growth factor (33). High levels of cyclin D1 in proliferating nontransformed lung type II-like cells has been described previously (34). Upregulation of cyclin D1 after EGFR activation in this cell type may not have been reported, although an increase in cyclin D1 in primary rat type II cells was noted after treatment with keratinocyte growth factor (35).

A novel and interesting aspect of our findings relates to the connection between the EGFR and the PI3K downstream pathway

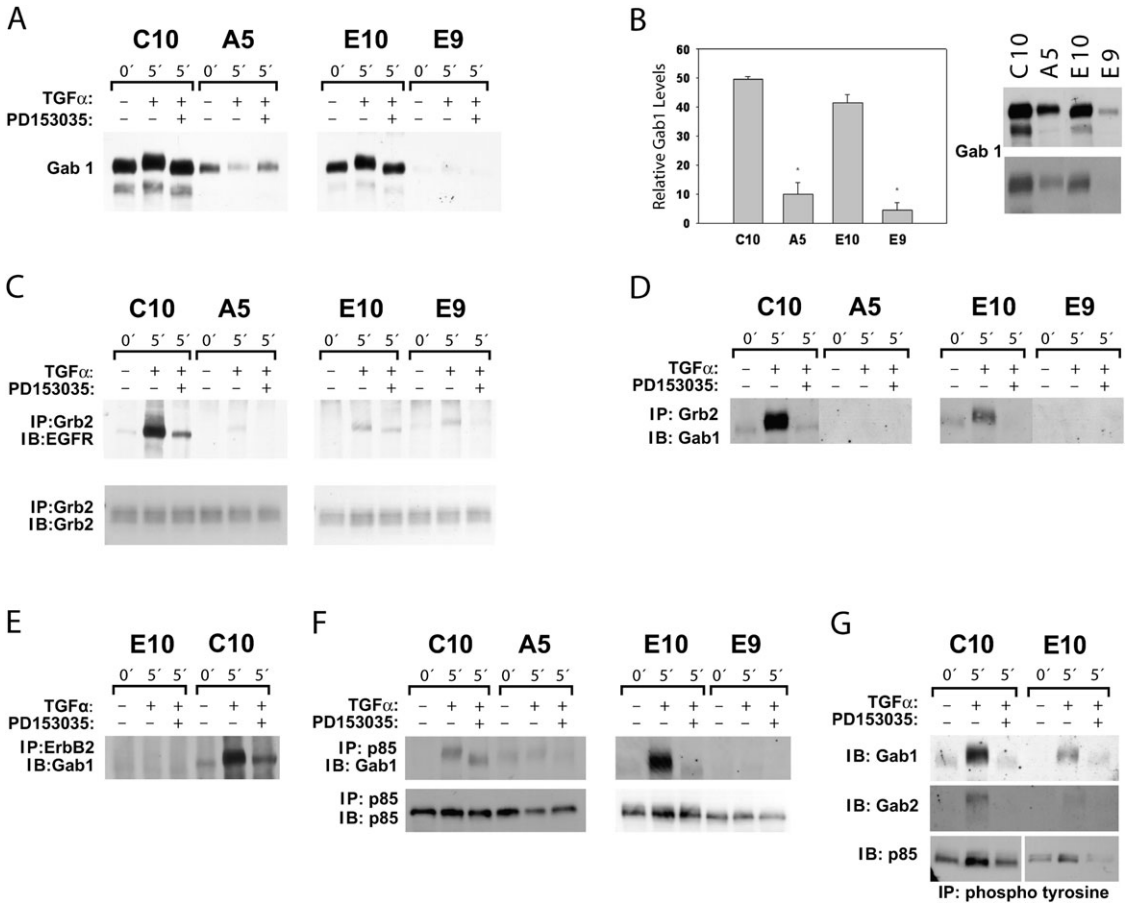

Figure 4. High levels of Gab1 and inducible Gab1/p85 complex in nontransformed E10 and C10 cells but not in E9 or A5 carcinoma cells. (*A*) Immunoblots for Gab1 in the four cell lines, serum starved and with TGF-α treatment with or without EGFR inhibitor PD153035. Much higher levels of Gab1 were found in C10 and E10 cells compared with A5 and E9 sister lines. Low levels of Gab1 were observed in E9 cells after longer exposure of the blot (not shown). A Gab1 mobility shift occurred in C10 and E10 after TGF-α treatment, suggestive of phosphorylation. (*B*) Quantification of the differing levels of Gab1 in the proliferating nontransformed versus proliferating malignant lung cells from three different experiments. Gab1 expression levels in A5 and E9 cells were significantly different from those in C10 and E10, respectively ($P < 0.01$). Two exposure levels of a representative western blot of Gab1 are shown. (*C*) C10, A5, E10, and E9 cells were treated as described previously, immunoprecipitated with anti-Grb2, and immunoblotted for EGFR (6% gel). Increased levels of EGFR coimmunoprecipitated with Grb2 in all four TGF-α–treated cells. A weak band was observed for A5 cells after longer exposure of the blot (not shown). PD 153035 treatment inhibited the association of EGFR with Grb2. Lysates immunoprecipitated with anti-Grb2 were resolved in 12% gel and immunoblotted with Grb2 (*middle panel*). (*D*) Cell lysates immunoprecipitated with anti-Grb2 were immunoblotted for Gab1. Large amounts of this complex were formed in response to TGF-α stimulation in C10 and E10 cells and completely blocked with PD153035. No Grb2-Gab1 complexes were detectable in E9 and A5 cells. (*E*) C10 and E10 cells were treated as described previously, and 1 mg cell lysate from each cell line was immunoprecipitated with anti-ErbB2 and immunoblotted with anti-Gab1. TGF-α induced direct association of ErbB2/Gab1 complex only in C10 cells. Inhibitor PD153035 blocked this association. (*F*) Immunoprecipitation of lysates of TGF-α–stimulated C10 and E10 cells with anti-p85 contained substantial amounts of immunoblotted Gab1; less Gab1 and with a different migration pattern was seen when the EGFR inhibitor PD153035 was used. No Gab1 signal was observed in E9 cells. A low level of constitutive p85/Gab1 complex in A5 cells was decreased after TGF-α treatment and was absent with PD153035 treatment. (*G*) Lysates of C10 and E10 cells were immunoprecipitated with antiphosphotyrosine after treatment with TGF-α with or without PD153035 and immunoblotted sequentially with stripping, anti-Gab1, anti-Gab2, and anti-p85. The presence of immunoblotted Gab2 in the complex in E10 cells was confirmed by a longer exposure of the blot (not shown). Inhibitory effects of PD153035 confirmed EGFR-dependent increases in Gab1, Gab2, and p85 in the immunoprecipitates.

leading to cell-cycle enhancement. This connection seemed to differ in the cancer cell lines compared with their nontransformed sister cell lines. The two cancer lines, E9 and A5, like their human counterparts (17), express high levels of ErbB3, which respond to activation of the EGFR to complex with ErbB2 and p85 of PI3K. The demonstrated high constitutive expression of TGF-α in these cells may result in a strong autocrine/paracrine stimulation of cell division. By contrast, the nontransformed sister lines, E10 and C10, do not express ErbB3 or TGF-α. Instead, they present Gab1, a multifunctional scaffolding adaptor, which is recruited to activated EGFR by the adaptor Grb2; PI3K is a prominent downstream target of activated Gab1 (21). We demonstrated in the E10 and C10 cells phosphorylation (activation) of Gab1 and formation of complexes with EGFR, Grb2, and p85 of PI3K in response to TGF-α. Shp2 was also present in these complexes. In the E9 and A5 cancer lines, on

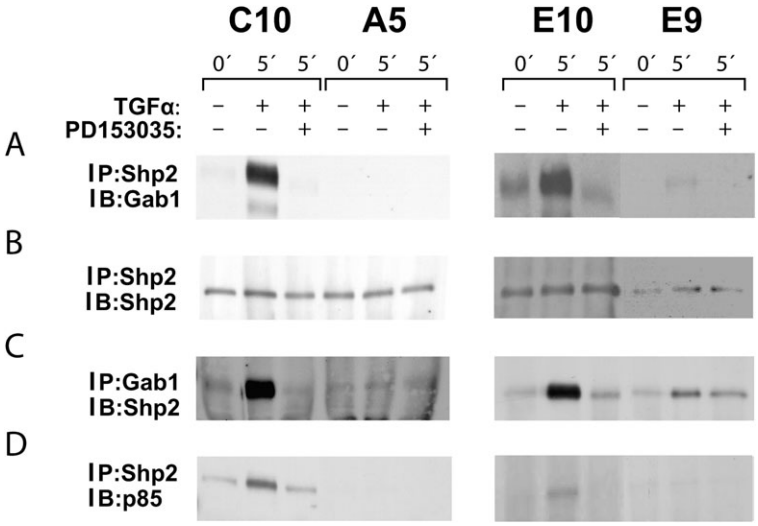

Figure 5. Complexes containing Shp2 with Gab1 and p85 in C10 and E10 cells. (*A* and *B*) C10/A5 and E10/E9 paired nontransformed/malignant cell lines were serum starved and treated with TGF-α with or without EGFR inhibitor PD153035. Lysates were immunoprecipitated with anti-Shp2 and immunoblotted sequentially with anti-Gab1 and anti-SHP2. In the nontransformed cells, the complex was increased in C10 and E10 cells by TGF-α, and this increase was blocked with PD153035. No Shp2/Gab1 containing complex was detectable in A5 cells; a low level was noted in E9 cells. (*C*) The four cell lines were treated as descibed previously, and lysates were immunoprecipitated with anti-Gab1 and immunoblotted with anti-Shp2. Results confirm the formation of a PD153035-inhibitable complex in the E10 and C10 cells, with much less in the A5 and none in the E9. (*D*) The four cell lines were treated as described previously, and lysates were immunoprecipitated with anti-Shp2 and immunoblotted with anti-p85. This complex was formed in response to TGF-α and was inhibited by PD153035 in C10 and E10 cells but not E9 and A5 cells.

the other hand, Gab1 complexes were minimal or absent and were not induced by TGF-α.

The occurrence of a complex containing Gab1 and ErbB2 is shown for the first time here. Although Gab1 has been shown to bind only to EGFR, it is possible that it can bind to other ErbB family receptors. Heregulin treatment, which induces only ErbB2/ErbB3 phosphorylation, stimulated Gab1 phosphorylation and associated PI3K activity in colon cancer cells (36). ErbB2 contains a putative Gab1 binding motif YXNQ at 1,139 in its carboxy terminus similar to that of ErbB1 at Y1068 (36). Recent reports have identified Gab1 as a downstream effector of ErbB2 (37–39). ErbB2-specific inhibitors have blocked the EGF-induced Gab1/PI3K/Akt pathway in colon cancer cells (33) and EGF-induced Gab1 phosphorylation in HEK 293 cells (40). Because EGF does not bind directly to ErbB2, these results suggest that Gab1 is activated downstream of ErbB2 possibly through EGFR/ErbB2 heterodimer activation.

Thus, although EGFR is a trigger for cell division in nontransformed and malignant PLE cells and PI3K and cyclin D1 are used in both situations, the membrane events that ensue immediately upon EGFR activation seem to differ, with ErbB2/ErbB3 recruitment occurring uniquely in the cancer cells but Grb2/Gab1 engaged and activated as a major pathway in the nontransformed cells only. It is tempting to speculate that the latter pathway can be regulated and turned on and off as part of normal cellular responses, whereas the former is autonomous and unresponsive to regulation when combined with TGF-α production. This is consistent with a view of Gab family proteins as signal amplifiers (21). It needs to be determined whether loss of Gab1 is essential to the establishment or maintenance of the malignant state and is thus a potential target for remedy. Consistent with our results, EGF induced an EGFR, Gab1, and Shp2 functional complex only in immortalized, nontumorigenic hamster embryo fibroblasts (41), whereas lack of Gab1 and functional loss of the EGFR, Gab1, Shp2 complex was noted in tumorigenic hamster embryo fibroblasts (41). Overexpression of a truncated Gab-1, unable to localize to the cell membrane, resulted in the enhancement of preneoplastic changes in hamster embryo fibroblasts (42).

On the other hand, Gab1 overexpression in murine fibroblasts promoted transformation (43), murine intestinal adenomas showed increased association of EGFR with Gab1 (44), and active ErbB2-mediated transformation of fibroblasts was blocked by Gab-1 knock-out (39). Efficient ErbB2 induced mammary tumor progression required EGFR-mediated Gab1 activation (38). In kidney cells, EGF activated Gab1 and Erk, and Erk caused downregulation of the active Gab1 via stimulation of a phosphatase (45). This suggests tight feedback regulation of Gab1. The degree of expression and the maintenance of regulation of Gab1 may be important to neoplasia development in various contexts.

The phosphatase Shp2 was present in the Gab1 complex in our nontransformed lung cells. An active role for Shp2 in Gab1 signaling has been apparent (20, 21) and is likely to be complex, at least in glioblastoma cells (46) and fibroblasts (43, 47). Multiple functions and possible contributions to cancer have been postulated for Shp2 (48). Failure of normal differentiation of lung was noted in Shp-$2^{-/-}$ chimeric mice, especially in those with a dysfunctional EGFR (49, 50). These findings support an important role for Shp2 downstream of EGFR in normal growth control in lung. No information on Gab1 is available for lung. Because the use of signaling molecules and pathways is cell-type specific changes in Gab-1 expression and function during lung tumorigenesis are worth further exploration.

In summary, our results indicate that activation of the EGFR of transformed and nontransformed PLE cells leads to upregulation of the cell cycle through events that include activation of PI3K and Akt and increased cyclin D1. However, the upstream connectors differ, with ErbB3 playing a key role in the cancer cells but with the adaptor Grb2, the docking protein Gab1, and the phosphatase Shp2 being prominent in the nontransformed cell lines. These data encourage therapeutic targeting of ErbB3 in lung adenocarcinomas and the development of strategies to enhance expression of Grb2/Gab1/Shp2 in these malignancies.

***Conflict of Interest Statement*:** None of the authors has a financial relationship with a commercial entity that has an interest in the subject of this manuscript.

***Acknowledgments*:** The authors thank Refika B. Turnier for flow cytometric analysis and Dr. Keith Kikawa for critical comments on this manuscript. The content of this publication does not necessarily reflect the views or policies of the Department of Health and Human Services, nor does mention of trade names, commercial products, or organizations imply endorsement by the U.S. Government.

References

1. Smith GJ, Le Mesurier SM, De Montfort ML, Lykke AWJ. Development and characterization of type 2 pneumocyte-related cell lines from normal adult mouse lung. *Pathology* 1984;16:401–405.

2. Bentel JM, Lykke AWJ, Smith GJ. Cloned murine non-malignant, spontaneously transformed and chemical tumor-derived cell lines related to the type 2 pneumocyte. *Cell Biol Int Rep* 1989;13:729–738.
3. Malkinson AM, Dwyer-Nield LD, Rice PL, Dinsdale D. Mouse lung epithelial cell lines: tools for the study of differentiation and the neoplastic phenotype. *Toxicology* 1997;123:53–100.
4. Olayioye MA, Neve RM, Lane HA, Hynes NE. The ErbB signaling network: receptor heterodimerization in development and cancer. *EMBO J* 2000;19:3159–3167.
5. Yarden Y, Sliwkowski MX. Untangling the ErbB signalling network. *Nat Rev Mol Cell Biol* 2001;2:127–137.
6. Aida S, Tamai S, Sekiguchi S, Shimizu N. Distribution of epidermal growth factor and epidermal growth factor receptor in human lung: immunohistochemical and immunoelectron-microscopic studies. *Respiration (Herrlisheim)* 1994;61:161–166.
7. Prigent SA, Lemoine NR, Hughes CM, Plowman GD, Selden C, Gullick WJ. Expression of the c-erbB-3 protein in normal human adult and fetal tissues. *Oncogene* 1992;7:1273–1278.
8. Yi ES, Harclerode C, Gondo M, Stephenson M, Brown RW, Younes M, Cagle PT. High c-erbB-3 protein expression is associated with shorter survival in advanced non-small cell lung carcinomas. *Mod Pathol* 1997;10:142–148.
9. Press MF, Cordon-Cardo C, Slamon DJ. Expression of the HER-2/*neu* proto-oncogene in normal human adult and fetal tissues. *Oncogene* 1990;5:953–962.
10. Rusch V, Baselga J, Cordon-Cardo C, Orazem J, Zaman M, Hoda S, McIntosh J, Kurie J, Dmitrovsky E. Differential expression of the epidermal growth factor receptor and its ligands in primary non-small cell lung cancers and adjacent benign lung. *Cancer Res* 1993;53:2379–2385.
11. Veale D, Ashcroft T, Marsh C, Gibson GJ, Harris AL. Epidermal growth factor receptors in non-small cell lung cancer. *Br J Cancer* 1987;55:513–516.
12. Rachwal WJ, Bongiorno PF, Orringer MB, Whyte RI, Ethier SP, Beer DG. Expression and activation of erbB-2 and epidermal growth factor receptor in lung adenocarcinomas. *Br J Cancer* 1995;72:56–64.
13. Poller DN, Spendlove I, Baker C, Church R, Ellis IO, Plowman GD, Mayer RJ. Production and characterization of a polyclonal antibody to the c-erbB-3 protein: examination of c-erbB-3 protein expression in adenocarcinomas. *J Pathol* 1992;168:275–280.
14. Lai WW, Chen FF, Wu MH, Chow NH, Su WC, Ma MC, Su PF, Chen H, Lin MY, Tseng YL. Immunohistochemical analysis of epidermal growth factor receptor family members in stage I non-small cell lung cancer. *Ann Thorac Surg* 2001;72:1868–1876.
15. Alimandi M, Romano A, Curia MC, Muraro R, Fedi P, Aaronson SA, Di Fiore PP, Kraus MH. Cooperative signaling of ErbB3 and ErbB2 in neoplastic transformation and human mammary carcinomas. *Oncogene* 1995;10:1813–1821.
16. Ram TG, Ethier SP. Phosphatidylinositol 3-kinase recruitment by p185erbB-2 and erbB-3 is potently induced by neu differentiation factor/heregulin during mitogenesis and is constitutively elevated in growth factor-independent breast carcinoma cells with c-erbB-2 gene amplification. *Cell Growth Differ* 1996;7:551–561.
17. Sithanandam G, Smith GT, Masuda A, Takahashi T, Anderson LM, Fornwald LW. Cell cycle activation in lung adenocarcinoma cells by the ErbB3/phosphatidylinositol 3-kinase/Akt pathway. *Carcinogenesis* 2003;24:1581–1592.
18. Sithanandam G, Fornwald LW, Fields J, Anderson LM. Inactivation of ErbB3 by siRNA promotes apoptosis and blocks growth and invasiveness of human lung adenocarcinoma cell line A549. *Oncogene* 2005;24:1847–1859.
19. McDoniels-Silver AL, Herzog CR, Tyson FL, Malkinson AM, You M. Inactivation of both Rb and p53 pathways in mouse lung epithelial cell lines. *Exp Lung Res* 2001;27:297–318.
20. Liu Y, Rohrschneider LR. The gift of Gab. *FEBS Lett* 2002;515:1–7.
21. Gu H, Neel BG. The 'Gab' in signal transduction. *Trends Cell Biol* 2003;13:122–130.
22. Brognard J, Clark AS, Ni Y, Dennis PA. Akt/protein kinase B is constitutively active in non-small cell lung cancer cells and promotes cellular survival and resistance to chemotherapy and radiation. *Cancer Res* 2001;61:3986–3997.
23. Lin X, Bohle AS, Dohrmann P, Leuschner I, Schulz A, Kremer B, Fandrich F. Overexpression of phosphatidylinositol 3-kinase in human lung cancer. *Langenbecks Arch Surg* 2001;386:293–301.
24. Tsao AS, McDonnell T, Lam S, Putnam JB, Bekele N, Hong WK, Kurie JM. Increased phospho-AKT(Ser^{473}) expression in bronchial dysplasia: implications for lung cancer prevention studies. *Cancer Epidemiol Biomarkers Prev* 2003;12:660–664.
25. Sordella R, Bell DW, Haber DA, Settleman J. Gefitinib-sensitizing EGFR mutations in lung cancer activate anti-apoptotic pathways. *Science* 2004;305:1163–1167.
26. Mukohara T, Kudoh S, Matsuura K, Yamauchi S, Kimura T, Yoshimura N, Kanazawa H, Hirata K, Inoue K, Wanibuchi H, *et al.* Activated Akt expression has significant correlation with EGFR and TGF-alpha expressions in stage I NSCLC. *Anticancer Res* 2004;24:11–17.
27. Chess PR, Ryan RM, Finkelstein JN. Tyrosine kinase activity is necessary for growth factor-stimulated rabbit type II pneumocyte proliferation. *Pediatr Res* 1994;36:481–486.
28. Ryan RM, Mineo-Kuhn MM, Kramer CM, Finkelstein JN. Growth factors alter neonatal type II alveolar epithelial cell proliferation. *Am J Physiol* 1994;266:L17–L22.
29. Zeng Q, Qian Z, Su T, Sun Q, Jiang H. The effects of transforming growth factor alpha and beta1 on the proliferation of alveolar type II cells in vitro. *Zhonghua Bing Li Xue Za Zhi* 1999;28:432–435.
30. Rice PL, Porter SE, Koski KM, Ramakrishna G, Chen A, Schrump D, Kazlauskas A, Malkinson AM. Reduced receptor expression for platelet-derived growth factor and epidermal growth factor in dividing mouse lung epithelial cells. *Mol Carcinog* 1999;25:285–294.
31. Manning CB, Cummins AB, Jung MW, Berlanger I, Timblin CR, Palmer C, Taatjes DJ, Hemenway D, Vacek P, Mossman BT. A mutant epidermal growth factor receptor targeted to lung epithelium inhibits asbestos-induced proliferation and proto-oncogene expression. *Cancer Res* 2002;62:4169–4175.
32. White MK, Strayer DS. Survival signaling in type II pneumocytes activated by surfactant protein-A. *Exp Cell Res* 2002;280:270–279.
33. Portnoy J, Curran-Everett D, Mason RJ. Keratinocyte growth factor stimulates alveolar type II cell proliferation through the ERK and PI3Kinase pathways. *Am J Respir Cell Mol Biol* 2004;30:901–907.
34. Mamay CL, Schauer IE, Rice PL, McDoniels-Silvers A, Dwyer-Nield LD, You M, Sclafani RA, Malkinson AM. Cyclin D1 as a proliferative marker regulating retinoblastoma phosphorylation in mouse lung epithelial cells. *Cancer Lett* 2001;168:165–172.
35. Buckley S, Driscoll B, Anderson KD, Warburton D. Cell cycle in alveolar epithelial type II cells: integration of Matrigel and KGF. *Am J Physiol* 1997;273:L572–L580.
36. Jackson JG, St Clair P, Sliwkowski MX, Brattain MG. Blockade of epidermal growth factor-or heregulin-dependent ErbB2 activation with the anti-ErbB2 monoclonal antibody 2C4 has divergent downstream signaling and growth effects. *Cancer Res* 2004;64:2601–2609.
37. Settle M, Gordon MD, Nadella M, Dankort D, Muller W, Jacobs JR. Genetic identification of effectors downstream of Neu (ErbB-2) autophosphorylation sites in a Drosophila model. *Oncogene* 2003;22:1916–1926.
38. Gillgrass A, Cardiff RD, Sharan N, Kannan S, Muller WJ. Epidermal growth factor receptor-dependent activation of Gab1 is involved in ErbB2-mediated mammary tumor progression. *Oncogene* 2003;22:9151–9155.
39. Yamasaki S, Nishida K, Yoshida Y, Itoh M, Hibi M, Hirano T. Gab1 is required for EGF receptor signaling and the transformation by activated ErbB2. *Oncogene* 2003;22:1546–1556.
40. Gensler M, Buschbeck M, Ullrich A. Negative regulation of HER2 signaling by the PEST-type protein-tyrosine phosphatase BDP1. *J Biol Chem* 2004;279:12110–12116.
41. Kameda H, Risinger JI, Han BB, Baek SJ, Barrett JC, Glasgow WC, Eling TE. Identification of epidermal growth factor receptor-Grb2-associated binder-1-SHP-2 complex formation and its functional loss during neoplastic cell progression. *Cell Growth Differ* 2001;12:307–318.
42. Kameda H, Risinger JI, Han BB, Baek SJ, Barrett JC, Abe T, Takeuchi T, Glasgow WC, Eling TE. Expression of Gab1 lacking the pleckstrin homology domain is associated with neoplastic progression. *Mol Cell Biol* 2001;21:6895–6905.
43. Holgado-Magruda M, Wong AJ. Role of the Grb2-associated binder 1/SHP-2 interaction in cell growth and transformation. *Cancer Res* 2004;64:2007–2015.
44. Moran AE, Hunt DH, Javid SH, Redston M, Carothers AM, Bertagnolli MM. Apc deficiency is associated with increased Egfr activity in the intestinal enterocytes and adenomas of C57BL/6J-Min/+ mice. *J Biol Chem* 2004;279:43261–43272.
45. Yu CF, Liu ZX, Cantley LG. ERK negatively regulates the epidermal growth factor-mediated interaction of Gab1 and the phosphatidylinositol 3-kinase. *J Biol Chem* 2002;277:19382–19388.
46. Kapoor GS, Zhan Y, Johnson GR, O'Rourke DM. Distinct domains in the SHP-2 phosphatase differentially regulate epidermal growth factor

receptor/NF-kappaB activation through Gab1 in glioblastoma cells. *Mol Cell Biol* 2004;24:823–836.
47. Mattoon DR, Lamothe B, Lax I, Schlessinger J. The docking protein Gab 1 is the primary mediator of EGF-stimulated activation of the PI-3K/Akt cell survival pathway. *BMC Biol* 2004;2:24.
48. Stein-Gerlach M, Wallasch C, Ullrich A. SHP-2, SH2-containing protein tyrosine phosphatase-2. *Int J Biochem Cell Biol* 1998;30:559–566.
49. Qu C-K, Yu W-M, Azzarelli B, Cooper S, Broxmeyer HE, Feng G-S. Biased suppression of hematopoiesis and multiple developmental defects in chimeric mice containing Shp-2 mutant cells. *Mol Cell Biol* 1998;18:6075–6082.
50. Qu C-K, Yu W-M, Azzarelli B, Feng G-S. Genetic evidence that Shp-2 tyrosine phosphatase is a signal enhancer of the epidermal growth factor receptor in mammals. *Proc Natl Acad Sci USA* 1999;96:8528–8533.